INVESTIGATION OF HEAT LOSSES FROM THE TRAPEZOIDAL CAVITY RECEIVER FOR LINEAR FRESNEL REFLECTOR SOLAR POWER SYSTEM

K. S. Reddy*, K. Ravi Kumar

Heat Transfer and Thermal Power Laboratory,

Department of Mechanical Engineering

Indian Institute of Technology Madras, Chennai-600036, India

* Email: ksreddy@iitm.ac.in (K.S. Reddy), Tel.: +91-44-22574702, Fax: +91-44-22574652

Abstract

Medium and high temperature heat can be produced by using concentrating solar power (CSP) technologies. Among CSP technologies, linear Fresnel reflector (LFR) system is simple in design and cost effective technology for medium temperature (400 ^{o}C) applications. In this article, the numerical investigation of the receiver for LFR system is carried out to estimate the combined convective and radiative heat losses. The 2-D numerical simulation of trapezoidal cavity receiver is carried out using commercial CFD package, Fluent – 6.3. The cavity receiver surface absorbs maximum amount of reflected solar radiation with minimum heat losses. At steady state conditions, the cavity receiver surface will attain almost uniform temperature; therefore, an isothermal boundary condition and also Boussinesq approximation are considered in the numerical simulations. To account the radiation exchange between the surfaces, the surface-to-surface model is used. The heat loss analyses are carried out for various receiver geometric and operating parameters viz. aspect ratio (ratio of receiver aperture to receiver width), cavity depth and width, operating temperature and wind speed. Based on the numerical analysis of the receiver, an optimum configuration of the receiver is found at insulation thickness of 300 mm, cavity depth of 300 mm with an aspect ratio of 2. The total heat loss varies from 614.32 W/m to 968.8 W/m for absorber width of 300 mm to 800 mm at 500 ^{o}C receiver temperature, 0.5 cavity cover emissivity and 2.5 m/s wind velocity. The effect of cavity cover emissivity on total heat loss is found to be less significant when compared to that of other cavity parameters. The optimum configuration of the inverted trapezoidal cavity receiver is arrived based on the heat loss analysis of the receiver.

Keywords: Solar energy, Linear Fresnel reflector, Cavity receiver, Heat loss, FLUENT

1. Introduction

Solar energy has the greatest potential among all the renewable energy sources. The medium and high temperature heat can be produced by using concentrating solar technologies. Based on the reflector configurations, the solar concentrating technologies may be classified as: linear Fresnel reflector, parabolic trough, parabolic dish and power tower. Among these, the linear Fresnel reflector (LFR) system is simple in design and cost effective system for medium temperature (100 ^{o}C – 400 ^{o}C) applications. The performance of the LFR system significantly depends on the design of the receiver. The design and performance evaluation of the receiver for linear Fresnel reflector system have been reported by the earlier researchers. Negi et al. (1990) presented the optical design and performance characteristics of a linear Fresnel reflector with a flat vertical absorber. The analysis has been carried out to study the effect of absorber height, concentrator aperture diameter and receiver width on performance of the system. The development and performance of linear Fresnel concentrating system with different sets of mirrors have been carried out by Singh et al. (1999). Mills and Morrison (2000) evaluated the compact linear Fresnel reflector (CLFR) system for large scale solar thermal power plants. Alternative versions of the basic CLFR concept have been evaluated interms of receiver and

reflector field configurations. Reynolds et al. (2002) developed heat loss and hydrodynamic models for CLFR system to predict output steam conditions and pressure drop across the receiver tubes for given input and environment conditions. Pye et al. (2003) developed correlations for unsteady heat losses from the receiver of CLFR system and compared with the steady state conditions.

Dey (2004) carried out analysis to maximize the heat transfer between the absorbing surface and the receiver tubes. Reynolds et al. (2004) studied the heat loss characteristics of trapezoidal cavity receiver for linear Fresnel reflector system. The heat losses from the receiver and the flow visualization technique to capture the flow patterns within the cavity have been described. Mills et al. (2004) proposed the CLFR system for feed water heating of 35 MW_e coal fired power plant. Eck et al. (2007) analyzed the thermal mass of receiver tubes for horizontal linear Fresnel collectors. The highest thermal mass was found out in the superheating section due to the lowest heat transfer coefficient at the inner surface of the absorber tube. Mills and Morrison (2007) analyzed the performance and cost of the compact Fresnel reflector power plants for large scale solar thermal power generation. The flux distribution of linear Fresnel reflector system was analyzed by Reddy and Reddy (2009). Based on the flux distribution analysis, receiver size was optimized for maximum energy capture and the concentration ratio of the system was determined.

The receiver is one of the important components in the linear Fresnel reflector power system. The design of the receiver significantly influences the overall performance of the system. The convective and radiative heat transfer in the cavity has been studied by several researchers. Natarajan et al. (2008) investigated the natural convection in the trapezoidal cavity with uniformly and non-uniformly heated bottom wall. Reddy and Kumar (2008) studied the combined natural convection and surface radiation heat transfer in a cavity receiver for the solar parabolic dish collector. The influence of various parameters such as operating temperature, emissivity of the surface, orientation and the geometry on total heat loss have been investigated. Reddy and Kumar (2009) investigated convection and surface radiation heat losses from the cavity receiver with different secondary reflectors. Basak et al. (2009) simulated the natural convection within the trapezoidal enclosures for uniformly heated bottom wall, linearly heated vertical walls and insulated top wall. Facao and Oliveira (2011) analyzed the natural convection inside the cavity receiver and optimized the cavity geometric parameter such as cavity depth and insulation thickness. Most of the above studies dealt with natural convection and radiation heat transfer separately in the cavity but only few studies are available for combined natural convection and radiation heat loss from the trapezoidal cavity with simplified form. In this article, an attempt has been made to evolve optimum configuration of the receiver based on the combined convective and radiative heat losses from the inverted trapezoidal cavity receiver with actual convective and radiative boundary conditions.

2. Modeling of solar linear Fresnel reflector power system

2.1. System description

The linear Fresnel reflector system comprises of array of long parallel curved/flat mirrors/reflectors and focal cavity receiver. The reflectors are equipped with single axis tracking, to focus the solar radiation onto the focal cavity receiver. The schematic of the linear Fresnel reflector with inverted trapezoidal cavity receiver is shown in Fig. 1. The receiver is placed at the middle of the module at the focal distance to absorb maximum solar radiation. The receiver consists of bank of black coated parallel high-pressure boiler grade tubes encased in an insulated inverted trapezoidal stainless steel cavity. The cavity aperture is covered with glass shield to allow concentrated solar radiation and to reduce heat losses from the cavity. The trapezoidal cavity is insulated with ceramic insulation to minimize heat losses and the insulation of the cavity is covered with mild steel casing. The parallel receiver tubes are placed very closely in the cavity to absorb the maximum concentrated solar radiation. In the present numerical modeling, it is assumed that the receiver tube surfaces equivalent to flat surfaces for the analysis and the cavity depth is considered from center of the receiver tubes to glass shield. The heat loss analyses are carried out for various receiver geometric and operating parameters viz. thickness of the insulation

(50 mm to 300 mm), aspect ratio (ratio of receiver width to receiver aperture, 1 to 3), cavity depth (100 mm to 400 mm), cavity width (300 mm to 800 mm), cavity cover emissivities (0 to 1), operating temperature (100 ^{o}C to 500 ^{o}C) and wind speed (0 m/s to 20 m/s) to arrive an optimum configuration. The thermo-physical properties of the cavity receiver are illustrated in Table. 1.

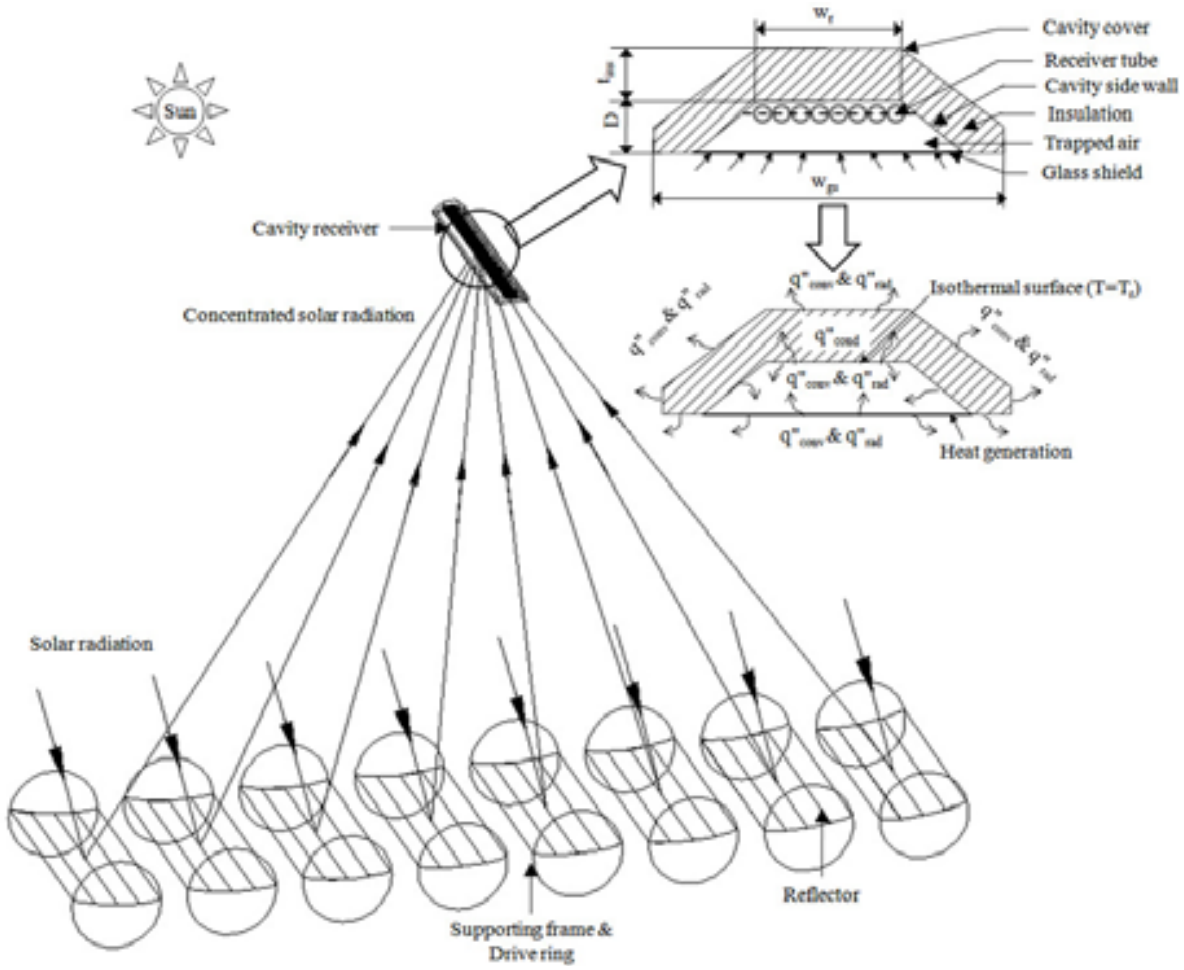

Fig. 1: Schematic of linear Fresnel reflector system

Tab. 1: Thermo-physical properties of cavity, insulation and glass shield

Property	Cavity absorber	Insulation	Glass Shield
Material	Steel	Ceramic Fiber	Borosilicate
Density (kg m^{-3})	8030	60	2230
Specific heat (J kg^{-1} K^{-1})	502.48	670	837.36
Thermal conductivity (W m^{-1} K^{-1})	16.27	0.04	1.46
Transmissivity	-	-	0.92
Absorptivity	-	-	0.034

2.2. Modeling of the inverted trapezoidal cavity receiver

The numerical simulations have been carried out to investigate the convective and radiative heat losses from the inverted trapezoidal cavity receiver for different receiver geometric and operating parameters. The flow and heat transfer simulations in the cavity receiver are carried out by solving mass, momentum and energy equation simultaneously. The continuity, momentum and energy equations is given as (Yuan, 1988):

Continuity equation

$$\frac{\partial u}{\partial x}+\frac{\partial v}{\partial y}=0 \qquad \text{(eq. 1)}$$

X - Momentum equation

$$u\frac{\partial u}{\partial x}+v\frac{\partial u}{\partial y}=-\frac{1}{\rho}\frac{\partial p}{\partial x}+\upsilon\left(\frac{\partial^2 u}{\partial x^2}+\frac{\partial^2 u}{\partial y^2}\right) \qquad \text{(eq. 2)}$$

Y - Momentum equation

$$u\frac{\partial v}{\partial x}+v\frac{\partial v}{\partial y}=-\frac{1}{\rho}\frac{\partial p}{\partial y}+\upsilon\left(\frac{\partial^2 v}{\partial x^2}+\frac{\partial^2 v}{\partial y^2}\right)+F_{By} \qquad \text{(eq. 3)}$$

Energy equation

$$u\frac{\partial T}{\partial x}+v\frac{\partial T}{\partial y}=\alpha\left(\frac{\partial^2 T}{\partial x^2}+\frac{\partial^2 T}{\partial y^2}\right)+\upsilon\frac{\partial^2 u}{\partial y^2} \qquad \text{(eq. 4)}$$

The continuity, momentum and energy equations are used to solve the convection model. The surface-to-surface (S2S) model has been used to account the radiation exchange along with the convection (Reddy and Kumar, 2008). The energy exchange by radiation between two surfaces depends on their shape, size and distance between the two surfaces. The radiant flux from a given surface involves two components, emitted and reflected energy. The reflected energy flux depends on incident energy flux from the surroundings, which can be expressed in terms of energy leaving from all other surfaces. The energy reflected from i^{th} surface is given as (Modest, 2003):

$$q''_{out,i}=\varepsilon_i\sigma T_i^4+\left(1-\varepsilon_i\right)q''_{in,i} \qquad \text{(eq. 5)}$$

The amount of incident energy upon a surface from another surface is a direct function of surface-to-surface view factor F_{ji}. The incident energy flux $q''_{in,i}$ can be expressed in terms of energy flux leaving from all other surfaces as:

$$A_i q''_{in,i}=\sum_{j=1}^{N}A_j q''_{out,j}F_{ji} \qquad \text{(eq. 6)}$$

For N surfaces, view factor reciprocity theorem gives

$$A_j F_{ji}=A_i F_{ij} \qquad \text{(eq. 7)}$$

Therefore, $q''_{in,i}$ is expressed as:

$$q''_{in,i}=\sum_{j=1}^{N}F_{ij}q''_{out,j} \qquad \text{(eq. 8)}$$

Substituting equation (8) in equation (5)

$$q''_{out,i} = \varepsilon_i \sigma T_i^4 + (1-\varepsilon_i) \sum_{j=1}^{N} F_{ij} q''_{out,j} \quad \text{(eq. 9)}$$

The equation (9) can be rewritten as

$$J_i = E_i + (1-\varepsilon_i) \sum_{j=1}^{N} F_{ij} J_j \quad \text{(eq. 10)}$$

2.3 Boundary conditions

The receiver surface is continuously exposed to concentrated solar radiation. At steady state condition, the cavity surface may attain uniform temperature; therefore isothermal boundary condition is applied on the receiver surface. The receiver surface is coated with selective coating to absorb maximum solar radiation and to reduce reradiating losses. Therefore, emissivity of the receiver surface is considered as 0.1. The cavity side walls absorb heat from the receiver surface by convection and radiation. The cavity side walls give heat to glass shield by convection and radiation and to cavity outside surface by conduction through insulation. Therefore, the cavity side walls are subjected to conductive, convective and radiative boundary conditions. Cavity glass shield is heated up by convection and re-radiation from the receiver surface and cavity side walls. Also cavity glass shield is heated up by absorbing concentrated solar radiation due to its absorptivity. The absorptivity and emissivity of the borosilicate glass shield is considered as 0.034 and 0.9 respectively. The glass shield is subjected to convective and radiative boundary conditions along with heat generation. The cavity outer cover surface includes bottom horizontal wall, vertical wall, outside inclined wall and outside top wall are exposed to ambient and it gives heat to the ambient and is subjected to convective and radiative boundary conditions. The inverted trapezoidal receiver is surrounded by infinite atmosphere. The flow of air is considered as flow across the receiver. The left side wall of the ambient domain is considered as inlet and is subjected to uniform velocity boundary condition. The right side wall is considered as outlet and is subjected to pressure outlet condition. The top and bottom wall of the ambient domain is considered as pressure inlet conditions.

The following assumptions have been made in the present numerical analysis (a) the receiver plane temperature is assumed as the surface temperature of the receiver tubes and it is uniform throughout the cavity width (b) the internal surfaces of the receiver are gray and diffuse (c) air is assumed as non-participating media for the radiation analysis (d) emissivity of the receiver and glass shield is considered as 0.1 and 0.9 respectively.

2.4 Estimation of heat losses from trapezoidal cavity receiver

The convective and radiative heat losses from the inverted trapezoidal cavity receiver have been investigated for different receiver operating temperatures, aspect ratios, insulation thickness, cavity width, cavity depth, emissivities of the cavity cover surface and wind velocities. The convective and radiative heat losses from the cavity can be calculated by estimating the total and radiative heat transfer from the surface or by estimating the total and radiative heat transfer coefficients and surface temperature of the cavity. The total heat transfer coefficient can be written as:

$$h_t = \frac{Q_t}{A(T_{out} - T_a)} \quad \text{(eq. 11)}$$

Also, total heat loss from the inverted trapezoidal cavity receiver can be calculated as

$$Q_t = Q_{conv} + Q_{rad} \quad \text{(eq. 12)}$$

The radiative heat transfer can be calculated by

$$Q_{rad} = h_{rad} A\left(T_{out} - T_a\right) \quad \text{(eq. 13)}$$

$$\text{where, } h_{rad} = \varepsilon\sigma\left[\frac{T_{out}^4 - T_a^4}{T_{out} - T_a}\right]$$

Convective heat loss from the cavity receiver surface can be calculated as

$$Q_{conv} = h_{conv} A\left(T_{out} - T_a\right) \quad \text{(eq. 14)}$$

$$\text{where, } h_{conv} = h_t - h_{rad}$$

3. Results and Discussion

3.1 Numerical Procedure

The 2-D numerical simulations of trapezoidal heat loss analyses have been carried out using commercial computational fluid dynamics software, Fluent-6.3 (Fluent Inc., 2006). The inverted trapezoidal receiver is surrounded by infinite atmosphere. The atmosphere (ambient domain) is considered for the analysis and its size is increased until the variation in heat loss is insignificant. In the present analysis, outer domain size is considered 10 times that of cavity receiver. The governing equations are solved using finite volume method by segregated implicit solver. Boussinesq approximation is enabled while solving the momentum equation, considering air as a working fluid. To account the radiation exchange between the surfaces, S2S model has been used (Reddy and Kumar, 2008). In the discretization scheme, body force weighted average has been used for pressure and SIMPLEC algorithm has been used for pressure-velocity coupling. The second order upwind differencing scheme is used for momentum and energy equations. The normalized residuals are considered as 10^{-3} for mass, momentum and 10^{-6} for energy equations for converging solution sufficiently. The grid independent study has been carried out before the actual simulation of inverted trapezoidal receiver. It is found that, 710250 cells are sufficient with minimum deviation of Nusselt number with the previous values of the cavity receiver.

The present numerical procedure is validated with heat loss from the trapezoidal cavity receiver for linear Fresnel reflector developed by Pye (2008). The comparison of total heat losses from the cavity receiver of Pye model (2008) and present numerical procedure has been carried out and it is found that the present numerical procedure deviates maximum of ±10.1%. Therefore the present numerical procedure has been used for the heat loss analyses of inverted trapezoidal cavity receiver.

3.2 Cavity parameter study

The heat losses from the trapezoidal cavity receiver are analyzed for various geometric and operating parameters of the receiver.

3.2.1 Cavity geometry parameters

The insulation thickness ranging from 50 mm to 300 mm, aspect ratio (ratio of receiver width to receiver aperture) ranging from 1 to 3, cavity depth ranging from 100 mm to 400 mm, cavity width ranging from 300 mm to 800 mm, cavity cover emissivities ranging from 0 to 1, operating temperature ranging from 100 ^{o}C to 500 ^{o}C and wind speed ranging from 0 m/s to 20 m/s to arrive an optimum configuration. The glass shield is considered at the bottom of inverted trapezoidal cavity receiver with an emissivity and absorptivity as 0.9 and 0.034 respectively. The glass shield absorbs part of incoming concentrated solar radiation and the rest is transmitted to the receiver surface. The emissivity of the receiver surface is assumed as constant and is considered to be 0.1.

The heat losses from trapezoidal cavity receiver are analyzed for different aspect ratio (A_s) and cavity depth (D) of the receiver with insulation thickness of 300 mm. Aspect ratio of the trapezoidal cavity receiver is defined as the ratio between the receiver aperture and the receiver width. The aspect ratio and cavity depth is varied from 1 to 3 and 100 mm to 400 mm respectively. The temperature contours of the cavity receiver for different aspect ratio when T_r = 500 ^oC, w_r = 0.5 m and D = 0.3 m is shown in Fig. 2. The cavity and glass shield temperature decreases with increase in aspect ratio. When the aspect ratio increases, the hot air gets trapped beneath the receiver. The glass shield and cavity cover total heat losses are found out for different aspect ratio and cavity depth and are shown in Fig. 3 and Fig. 4.

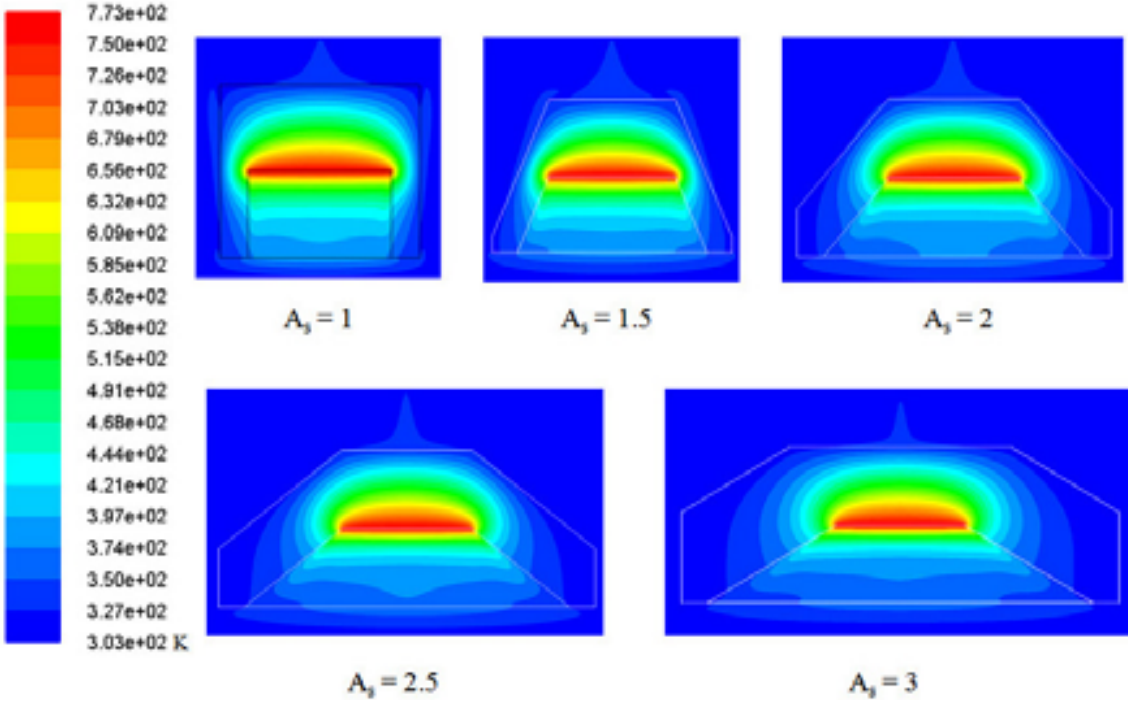

Fig. 2: Temperature contours of the cavity receiver for different aspect ratio when T_r = 500 ^oC and w_r = 0.5 m

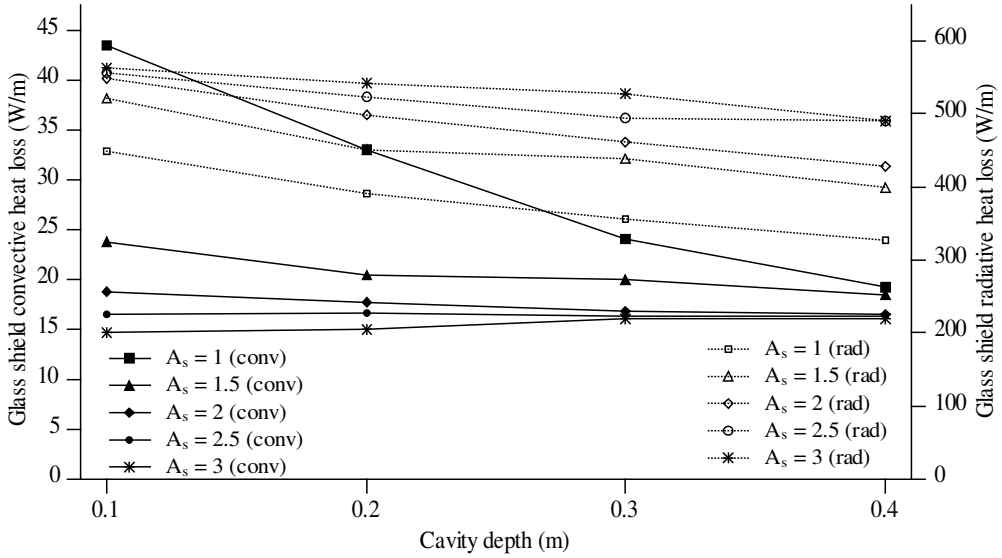

Fig. 3: Variation of glass shield convective and radiative heat losses with aspect ratio and cavity depth for T_r = 500 ^oC

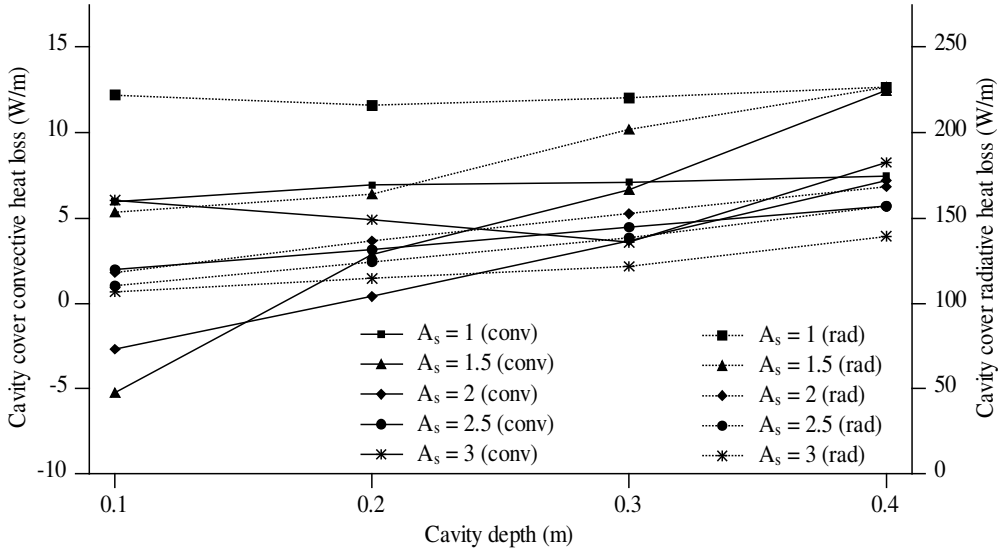

Fig. 4: Variation of cavity cover convective and radiative heat losses with aspect ratio and cavity depth for T_r = 500 °C

The combined (convective and radiative) heat losses from the glass shield decreases with increase in cavity depth. The convective heat losses from the cavity cover is negative for lower aspect ratios due to the amount of heat loss to the ambient is less than that of amount of heat absorbed from the hot air coming from beneath the glass shield. The combined cavity cover heat loss increases with cavity depth due to increase in cavity cover surface area. The combined glass shield heat losses increase with aspect ratio and cavity heat losses decrease with increase in aspect ratio. The variation of total combined glass shield and cavity heat losses from the receiver are significant till aspect ratio 2 and cavity depth 300 mm. But total combined heat losses are not significant beyond cavity depth of 300 mm and aspect ratio of 2.

The heat loss analyses are carried out for different receiver width varying from 300 mm to 800 mm with aspect ratio of 2, cavity depth of 300 mm and 300 mm insulation thickness. The variation of glass shield and cavity cover temperature with cavity width is shown in Fig. 5. The glass shield and cavity cover temperature decreases with increase in cavity width. The effect of cavity width on convective and radiative heat losses of glass shield and cavity cover is shown in Fig. 6. The variation of convective heat losses from the glass shield and cavity cover with cavity width is insignificant. The glass shield radiative heat loss is increases with cavity width due to glass shield aperture and temperature. Though glass shield temperature decreases with increase in cavity width, radiative heat losses increases; because, the effect of variation of temperature is less significant than variation of glass shield area.

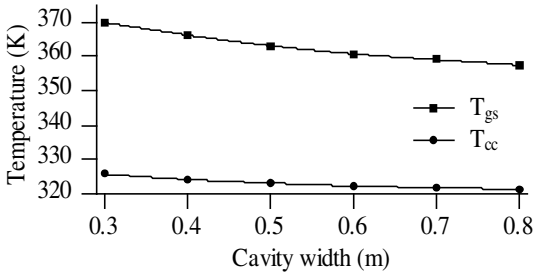

Fig. 5: Effect of cavity width on glass shield and cavity cover temperature for T_r = 500 °C

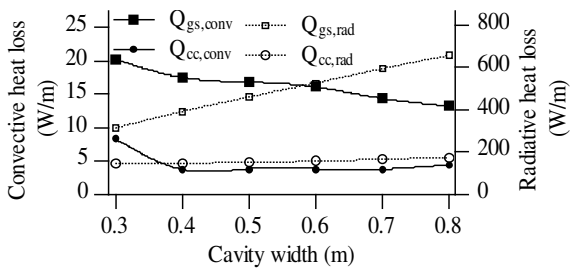

Fig. 6: Effect of cavity width on glass shield and cavity cover heat loss for T_r = 500 °C

The heat loss analyses are carried out by varying thickness of the insulation from 50 mm to 300 mm. Based on the IPSS (Inter Plant Standard Steel Industry) report, surface temperature of the cavity cover should not be 15 ^{o}C higher than that of ambient temperature when the receiver temperature is more than 400 ^{o}C at wind velocity of 1 m/s. The temperature difference between the cavity cover and ambient for different insulation thicknesses is shown in Fig. 7. The temperature difference decreases with increase in insulation thickness. The temperature difference is found as 14.1 ^{o}C when the insulation thickness is 300 mm at receiver temperature and wind velocity is 500 ^{o}C and 1 m/s respectively. Therefore, optimum thickness of the insulation is found to be 300 mm for the trapezoidal cavity receiver.

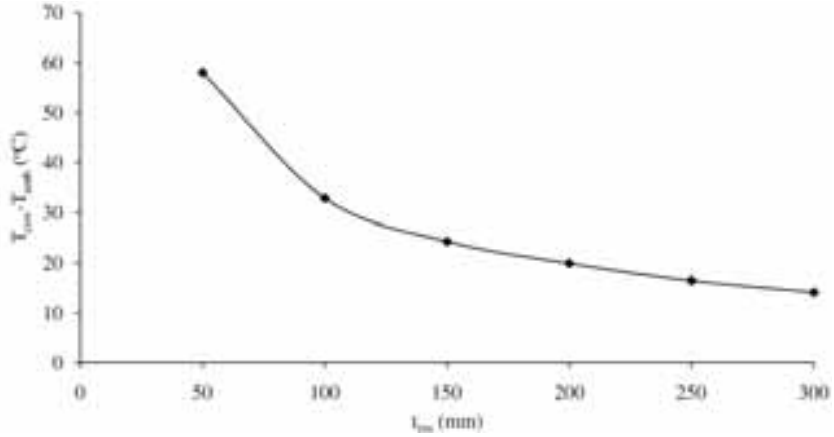

Fig. 7: Effect of insulation thickness on cavity cover temperature

3.2.2 Receiver temperature and wind velocity

The heat loss analyses are carried out for receiver temperature varying from 100 ^{o}C to 500 ^{o}C and wind velocity 0 m/s to 20 m/s with different cavity width. The effect of wind velocity on convective heat losses of glass shield and cavity cover is shown Fig. 8. The convective heat losses of glass shield and cavity cover increases with wind velocity. The variation of glass shield and cavity cover heat loss ratio (convective heat loss/radiative heat loss) with wind velocity is shown in Fig. 9. The heat loss ratio for both glass shield and cavity cover increases with wind velocity because more heat is carried by wind. The radiative heat losses of glass shield and cavity cover decreases with increase in wind velocity for all receiver temperature. This is due to glass shield and cavity cover temperature decreases with increase in wind velocity. The heat loss ratio decreases with increase in cavity width due to more radiative heat loss for higher cavity width than that of lower cavity width. The total heat losses from the cavity receiver is varying from 636 W/m to 951 W/m for wind velocity varying from 0 m/s to 20 m/s at the receiver temperature of 500 ^{o}C and receiver width of 500 mm. Based on the cavity heat loss analyses, the total heat losses vary between 263 W/m to 759 W/m for the receiver temperature varying between 100 ^{o}C to 500 ^{o}C for cavity width of 500 mm and wind velocity 2.5 m/s.

3.2.3 Cavity cover emissivity

The effect of cavity cover emissivity on cavity heat losses have been studied for different receiver temperatures for cavity width of 500 mm and wind velocity of 2.5 m/s. The cavity cover emissivity is varied from 0 to 1 in steps of 0.25. The effect of cavity cover emissivity on glass shield and cavity cover convective and radiative heat losses are shown in Fig. 10 and Fig. 11 respectively. The effect of cavity cover emissivity on glass shield convective and radiative heat losses is found to be negligible. The cavity cover convective heat losses decreases with increase in cavity cover emissivity and radiative heat losses increases with cavity cover emissivity.

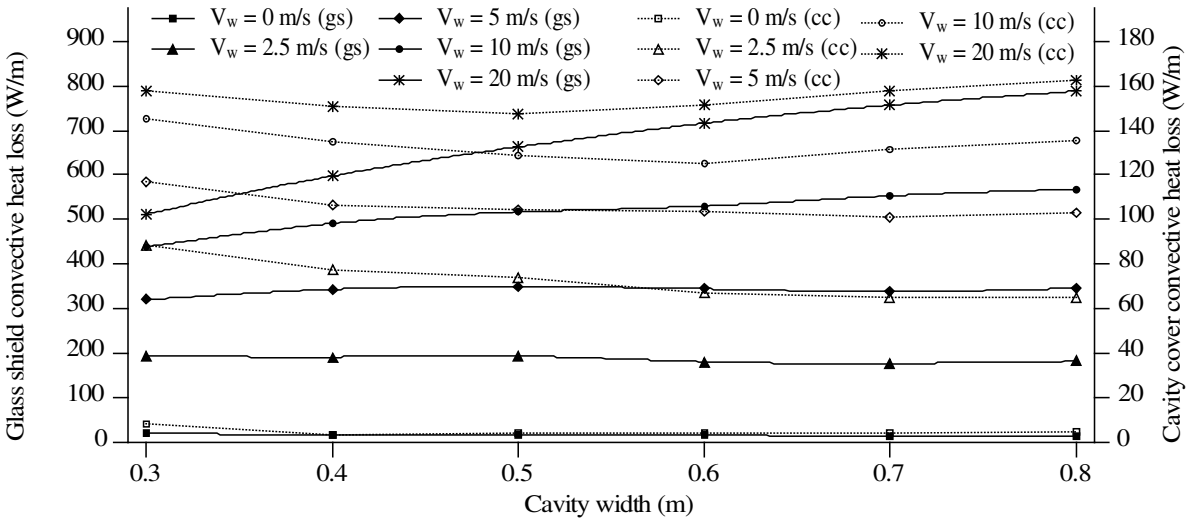

Fig. 8: Effect of wind velocity on glass shield and cavity cover convective heat loss for T_r = 500 °C

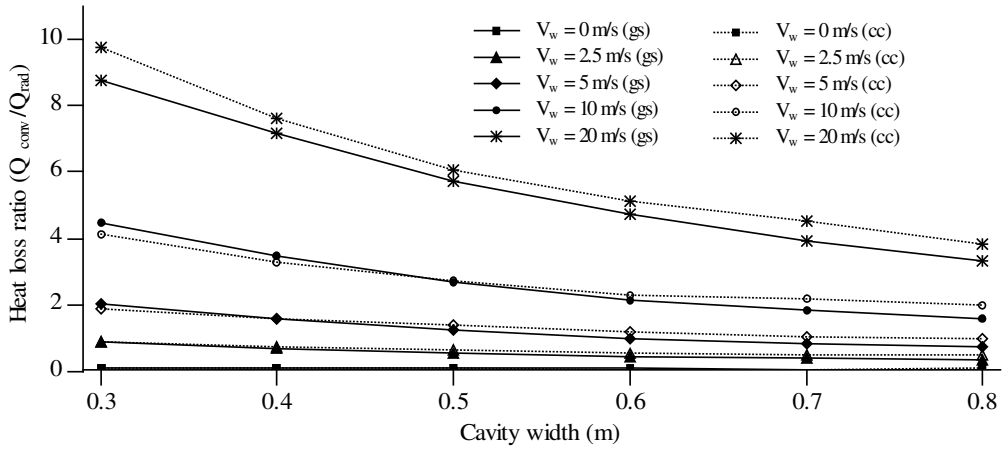

Fig. 9: Effect of wind velocity on glass shield and cavity cover heat loss ratio for T_r = 500 °C

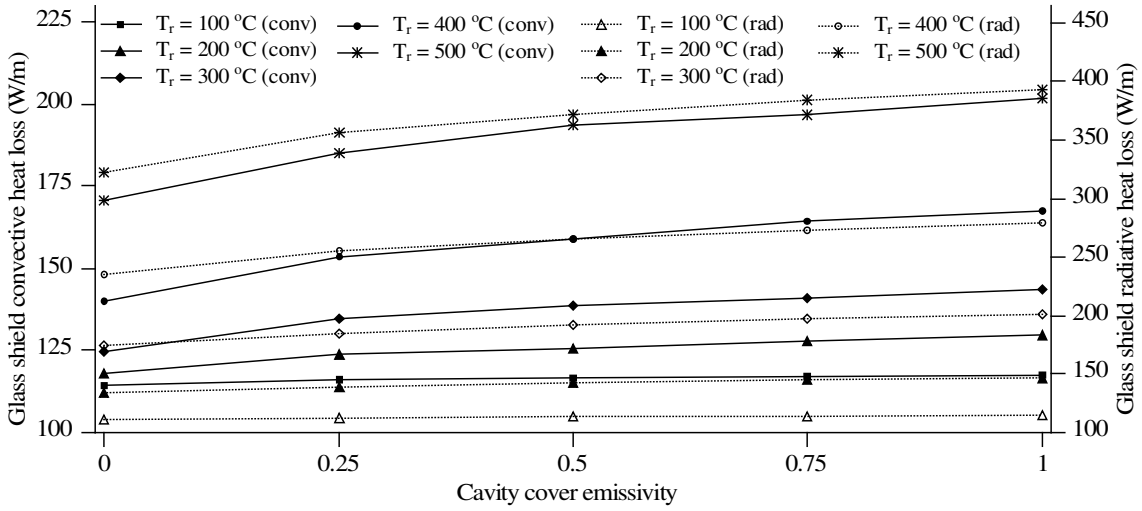

Fig. 10: Variation of glass shield convective and radiative heat loss with cavity cover emissivity for w_r = 0.5 m and V_w = 2.5 m/s

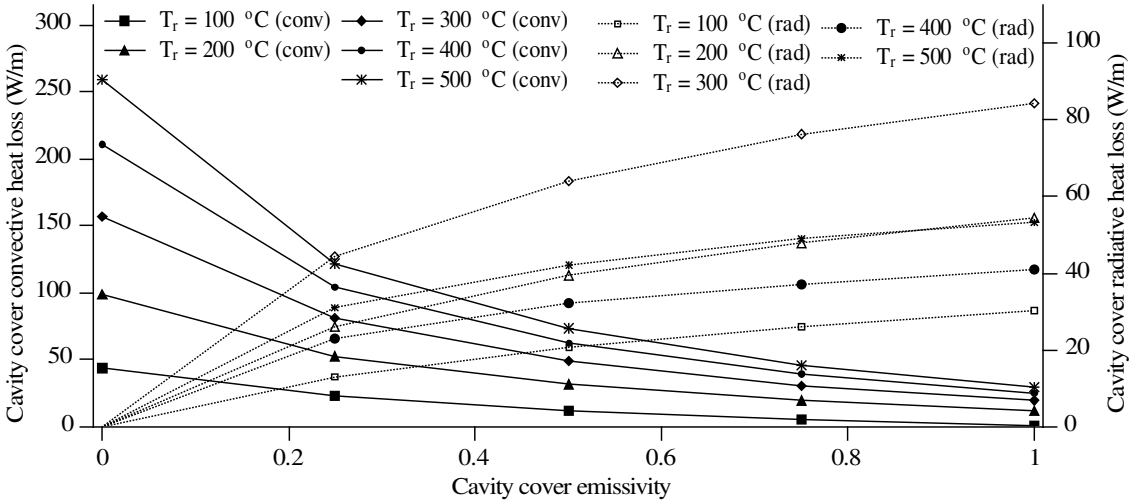

Fig. 11: Variation of cavity cover convective and radiative heat loss with cavity cover emissivity for w_r = 0.5 m and V_w = 2.5 m/s

4. Conclusions

The 2-D numerical simulations for combined convective and radiative heat losses from the inverted trapezoidal cavity receiver for linear Fresnel reflector solar power system have been carried out. Based on the numerical analyses of the receiver, optimum configuration is found for insulation thickness of 300 mm, cavity depth of 300 mm with an aspect ratio of 2. Though convective heat losses decrease with increase in receiver width due to hot air trapped beneath the cavity and radiative heat losses increase drastically with receiver width. The total convective heat loss decreases from 282.73 W/m to 246.65 W/m and total radiative heat losses increases from 331.58 W/m to 722.15 W/m when receiver width varies from 300 mm to 800 mm at 500 °C receiver temperature and 2.5 m/s wind velocity. Therefore, number of mirror rows has been designed carefully to minimize the total heat losses. Glass shield radiative heat losses from cavity receiver are significant compared to the other heat losses for all the given configurations. The analysis can be used to design an inverted trapezoidal cavity receiver for any capacity of linear Fresnel reflector power systems.

Nomenclature

A	area (m^2)
A_s	aspect ratio
D	cavity depth (m)
E	emissive power ($W\ m^{-2}$)
F	view factor
F_{By}	body force per unit volume in y direction ($N\ m^{-3}$)
h	heat transfer coefficient ($W\ m^{-2}\ K^{-1}$)
J	radiosity ($W\ m^{-2}$)
N	number of radiative surfaces
P	pressure ($N\ m^{-2}$)
q"	energy flux ($W\ m^{-2}$)
Q	heat loss (W)
T	temperature (°C)
t_{ins}	insulation thickness (m)
u, v	velocity ($m\ s^{-1}$)
V_w	wind velocity ($m\ s^{-1}$)
w	receiver width (m)
x, y	spatial position (m)

Greek symbols

α	thermal diffusivity ($m^2\ s^{-1}$)
ε	emissivity
ρ	density of the fluid ($kg\ m^{-3}$)
σ	Stefan-Boltzmann constant ($W\ m^{-2}\ K^{-4}$)
υ	kinematic viscosity ($m^2\ s^{-1}$)

Subscripts

a	ambient
cc	cavity cover
conv	convective
gs	glass shield
in	inlet
i, j	surfaces
out	outlet
r	receiver
rad	radiation
t	total

References

Balaji, C., Venkateshan, S.P., 1994. Correlations for free convection and surface radiation in a square cavity. Int. J. Heat and Fluid Flow, 15 (3), 249-251.

Basak, T., Roy, S., Singh, A., Pandey, B.D., 2009. Natural convection flow simulation for various angles in a trapezoidal enclosure with linearly heated side wall(s). Int. J. of Heat and Mass Transfer, 52, 4413–4425.

Dey, C.J., 2004. Heat transfer aspects of an elevated linear absorber. Solar Energy, 76, 243–249.

Eck, M., Uhlig, R., Mertins, M., Haberle, A., Lerchenmuller, H., 2007. Thermal load of direct steam-generating absorber tubes with large diameter in horizontal linear Fresnel collectors. Heat Transfer Engineering, 28(1), 42–48.

Facao, J., Oliveira, A.C., 2011. Numerical simulation of a trapezoidal cavity receiver for a linear Fresnel solar collector concentrator, Renewable Energy, 36, 90-96.

Fluent Inc., 2006. Fluent 6.3 user's guide. Lebanon: NH.

Mills, D.R., Morrison, G.L., 2000. Compact linear Fresnel reflector solar thermal power plants. Solar Energy, 68(3), 263–283.

Mills, D.R., Morrison, G.L., Lievre, P.L., 2004. Design of a 240 MW_e solar thermal power plant. In: Proceedings of the Eurosun 2004 Conference, June 20-24, Freiburg, Germany.

Mills, D.R., Morrison, G.L., 2007. Advanced Fresnel reflector power plants - performance and generating costs, Proceedings of ANZSES Solar 2007, Australia.

Modest, M.F., 2003. Radiative Heat Transfer. 2nd edn. Academic Press/Elsevier, USA, 162-175.

Natarajan, E., Basak, T., Roy, S., 2008. Natural convection flows in a trapezoidal enclosure with uniform and non-uniform heating of bottom wall, Int. J. of Heat and Mass Transfer, 51, 747–756.

Negi, B.S., Kandpal, T.C., Mathur, S.S., 1990. Designs and performance characteristics of a linear Fresnel reflector solar concentrator with a flat vertical absorber. Solar & Wind Technology, 7 (4), 379- 392.

Pye, J.D., Morrison, G.L., Behnia, M., 2003. Transient modelling of cavity receiver heat transfer for the compact linear Fresnel reflector. Proceedings of ANZSES Solar 2003, Melbourne.

Pye, J.D., 2008. System modelling of the compact linear Fresnel reflector. Ph. D thesis, University of New South Wales, Australia.

Reddy, K.S., Kumar, N.S., 2008. Combined laminar natural convection and surface radiation heat transfer in a modified cavity receiver of solar parabolic dish. Int. J. of Thermal Sciences, 47, 1647-1657.

Reddy, K. S., Kumar, N.S., 2009. Convection and surface radiation heat losses from modified cavity receiver of solar parabolic dish collector with two-stage concentration. Heat Mass Transfer. 45, 363–373.

Reddy, P.P.C., Reddy, K.S., 2009. Investigation of flux distribution on the receiver of solar linear Fresnel reflector power plant. 3rd International conference on Power Systems, December 27-29, 2009, IIT Kharagpur, India.

Reynolds, D.J., Behnia, M., Morrison, G.L., 2002. A hydrodynamic model for a line-focus direct steam generation solar collector. In: Proceedings of the ANZSES Solar 2002, Newcastle, Australia, 1-6.

Reynolds, D.J., Jance, M.J., Behnia, M., Morrison, G.L., 2004. An experimental and computational study of the heat loss characteristics of a trapezoidal cavity absorber. Solar Energy, 76, 229-234.

Singh, P.L., Ganesan, S., Yadav, G.C., 1999. Performance study of a linear Fresnel concentrating solar device. Renewable Energy, 18, 409-416.

Yuan, S.W., 1988. Foundations of Fluid Mechanics. 3rd edn. Prentice-Hall, London, 104-113.